

Reproducible bipolar resistive switching in entire nitride AlN/n-GaN metal-insulator-semiconductor device and its mechanism

Yiren Chen, Hang Song, Hong Jiang, Zhiming Li, Zhiwei Zhang, Xiaojuan Sun, Dabing Li, and Guoqing Miao

Citation: [Applied Physics Letters](#) **105**, 193502 (2014); doi: 10.1063/1.4901747

View online: <http://dx.doi.org/10.1063/1.4901747>

View Table of Contents: <http://scitation.aip.org/content/aip/journal/apl/105/19?ver=pdfcov>

Published by the [AIP Publishing](#)

Articles you may be interested in

[Unipolar resistive switching behavior of amorphous gallium oxide thin films for nonvolatile memory applications](#)
Appl. Phys. Lett. **106**, 042105 (2015); 10.1063/1.4907174

[Hydrothermal epitaxial growth and nonvolatile bipolar resistive switching behavior of LaFeO₃-PbTiO₃ films on Nb:SrTiO₃\(001\) substrate](#)
Appl. Phys. Lett. **105**, 152904 (2014); 10.1063/1.4898337

[Highly transparent bipolar resistive switching memory with In-Ga-Zn-O semiconducting electrode in In-Ga-Zn-O/Ga₂O₃/In-Ga-Zn-O structure](#)
Appl. Phys. Lett. **105**, 093502 (2014); 10.1063/1.4894521

[Bipolar resistive switching characteristics of low temperature grown ZnO thin films by plasma-enhanced atomic layer deposition](#)
Appl. Phys. Lett. **102**, 012113 (2013); 10.1063/1.4774400

[Analysis of AlN/AlGaIn/GaN metal-insulator-semiconductor structure by using capacitance-frequency-temperature mapping](#)
Appl. Phys. Lett. **101**, 043501 (2012); 10.1063/1.4737876

The advertisement features a photograph of the Model PS-100 cryogenic probe station, which is a complex piece of scientific equipment with various mechanical components and a probe. The background is a gradient of blue. The text is arranged around the image: the model name and description on the left, the company logo on the right, and a slogan at the bottom right.

Model PS-100
Tabletop Cryogenic
Probe Station

The logo for Lake Shore CRYOTRONICS consists of a stylized blue and white square icon to the left of the company name 'Lake Shore' in a large, white, serif font, with 'CRYOTRONICS' in a smaller, white, sans-serif font below it.

*An affordable solution for
a wide range of research*

Reproducible bipolar resistive switching in entire nitride AlN/n-GaN metal-insulator-semiconductor device and its mechanism

Yiren Chen, Hang Song,^{a)} Hong Jiang, Zhiming Li, Zhiwei Zhang, Xiaojuan Sun, Dabing Li,^{a)} and Guoqing Miao

State Key Laboratory of Luminescence and Applications, Changchun Institute of Optics, Fine Mechanics and Physics, Chinese Academy of Sciences, Changchun 130033, People's Republic of China

(Received 25 June 2014; accepted 3 November 2014; published online 10 November 2014)

Reproducible bipolar resistive switching characteristics are demonstrated in entire nitride AlN/n-GaN metal-insulator-semiconductor devices. The mechanism involved confirms to trap-controlled space charge limited current theory and can be attributed to the nitrogen vacancies of AlN serving as electron traps that form/rupture electron transport channel by trapping/detrapping electrons. This study will lead to the development of *in-situ* growth of group-III nitrides by metal-organic chemical vapor deposition as a candidate for next-generation nonvolatile memory device. Moreover, it will be benefit to structure monolithic integrated one-transistor-one-resistor memory with nitride high electron mobility transistors. © 2014 AIP Publishing LLC. [<http://dx.doi.org/10.1063/1.4901747>]

The traditional nonvolatile memory technology based on charge storage is rapidly approaching its fundamental scaling limit due to the increasing difficulty of reliably retaining sufficient electrons in shrinking dimensions.¹ In recent, memory concept based on resistive switching² rather than charge storage has inspired scientific and commercial attentions due to its simple architecture, high speed operation, high density integration, and good scalability.^{3,4} As the third generation of semiconductor, GaN-based materials which have been intensively studied for optoelectronic and microelectronic applications such as light-emitting diodes (LEDs),⁵ laser diodes,⁶ photodetectors,^{7,8} and high electron mobility transistors (HEMTs)⁹ are still in their early stage for memory devices. Moreover, there are few reports on resistive switching of GaN-based materials. The research on resistive memory devices based on GaN-based materials will be beneficial to structure monolithic integrated one-transistor-one-resistor (1T1R) memory with nitride HEMTs and fabricate a new generation of integrated memory device similar to Si-based materials.

So far, resistive switching, especially, bipolar resistive switching, has been extensively investigated in a large number of material systems, mainly including ferromagnetic materials,^{10,11} transition metal oxides,^{12,13} and organics,^{14,15} based on metal-insulator-metal (MIM) structure with different suggested mechanisms controlling switching as conducting filament, interfacial barrier, and interface state models.^{13,16-18} Nevertheless, the MIM structure is not suitable for structuring monolithic integrated 1T1R memory based on the entire nitride materials. Fortunately, the resistive switching is demonstrated in metal-insulator-semiconductor (MIS) structure besides in MIM structure. Cavallini *et al.*⁴ have observed reproducible resistive switching in metal/e-SiO₂/Si and ascribed the behavior to Si filament formed by electro-reductive/electromechanical process at negative bias and destroyed by oxidation at positive bias. Liu *et al.*¹⁹ have fabricated AlN film embedded with Al

nanoparticles on n-Si by radio frequency sputtering to obtain MIS device. It performed memory effect based on the mechanism of forming and breaking tunneling paths as a result of charging and discharging in the Al nanoparticles. Wu *et al.*²⁰ have found that oxygen vacancies as well as metallic filaments were responsible for the resistive switching in MIS device based on HfO₂-based high-k insulator. Chen *et al.*²¹ have demonstrated that the MIS device based on Al/ZnO/n-Si exhibited reproducible bipolar resistive switching effects and concerned the effects to the injection and extraction of the O²⁻ ions at the Al/ZnO interface, which resulted in the formation and dissolution of the AlO_x barrier layer. Although MIS devices fabricated by different materials presented bipolar resistive switching characteristics, the corresponding mechanisms proposed were not well suitable for our GaN-based materials.

In this letter, we grow AlN/n-GaN material using MOCVD and demonstrate reproducible bipolar resistive switching in AlN/n-GaN MIS device. Taking advantage of the characteristics, the nonvolatile memory device can be obtained based on GaN-based materials. The mechanism involved is also explicit and can be attributed to the nitrogen vacancies of AlN insulator serving as traps, which form/rupture electron transport channel by trapping/detrapping electrons. The process is in accordance with the trap-controlled space charge limited current (SCLC) theory.

The AlN/n-GaN material was grown on c-plane sapphire substrate by MOCVD. Trimethylgallium (TMGa), trimethylaluminum (TMAI), and ammonia (NH₃) were, respectively, used as Ga, Al, and N precursors while silane (SiH₄) as the n-type dopant. Prior to deposition, the surface of sapphire substrate was thermally desorbed under H₂ for 10 min at 1100 °C. Following the deposition of a 36-nm-thick GaN buffer layer at 550 °C, a 1- μ m-thick undoped GaN layer and a 200-nm-thick Si-doped GaN layer with carrier concentration of $\sim 2.5 \times 10^{18} \text{ cm}^{-3}$ were grown at 1050 °C. Then, the temperature was ramped up to 1100 °C for the deposition of AlN layer. The thickness of AlN layer was measured to be 80 nm in the cross-sectional image obtained by scanning

^{a)}Electronic addresses: songh@ciomp.ac.cn and lidb@ciomp.ac.cn

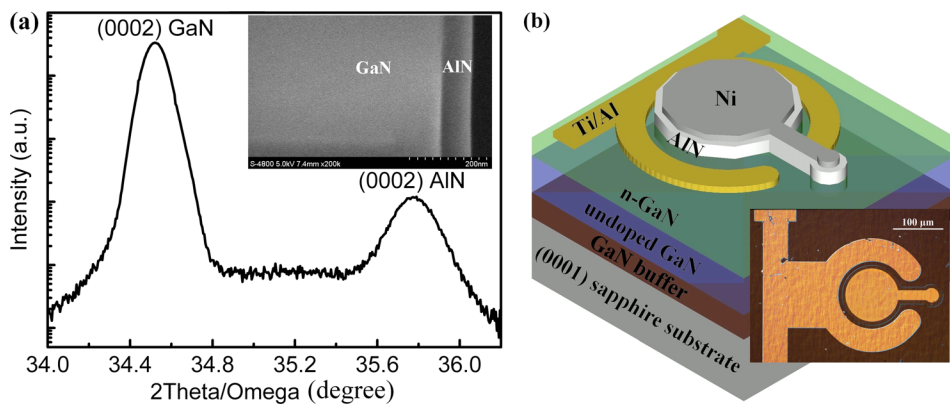


FIG. 1. (a) (0002) plane 2θ - ω scan of AlN/n-GaN by HRXRD. The inset shows its cross-sectional SEM image. (b) Schematic configuration of AlN/n-GaN MIS device. The inset shows the metallographic micrograph of a MIS cell.

electron microscope (SEM), as shown in the inset of Fig. 1(a). The AlN/n-GaN material had a single hexagonal phase, as demonstrated by (0002) plane 2θ - ω scan using high-resolution x-ray diffraction (HRXRD) in Fig. 1(a). In the subsequent process of fabricating the MIS structure device, an AlN mesa with diameter of $100\ \mu\text{m}$ was left by inductively coupled plasma (ICP) dry etching. Surrounding the mesa, a Ti/Al (50/150 nm) electrode was deposited onto the n-GaN layer using electron-beam evaporation and annealed at $700\ ^\circ\text{C}$ for 30 s in N_2 atmosphere to realize ohmic contact. On top of the AlN mesa, a Ni (300 nm) electrode was fabricated similarly and formed Schottky contact. The schematic configuration and metallographic micrograph of the MIS device were shown in Fig. 1(b).

Fig. 2(a) presents typical current-voltage (I - V) characteristic of the pristine AlN/n-GaN MIS device on semi-logarithmic scale, which is measured by Keithley 237 electrometer in piecewise continuous mode. The Ti/Al electrode on n-GaN is grounded, and the voltage applied to the top Ni electrode is swept in a sequence of $0\ \text{V} \rightarrow -8\ \text{V} \rightarrow 0\ \text{V} \rightarrow 4\ \text{V} \rightarrow 0\ \text{V}$, the directions indicated by red arrows are numbered from 1 to 4 in the inset of Fig. 2(a). By steadily decreasing the voltage from $0\ \text{V}$ to $-8\ \text{V}$ (arrow 1), a steep current rise is observed at about $-3\ \text{V}$. In this process, the device switches from high resistance state (HRS) to low resistance state (LRS), corresponding to the "SET" process. It retains at the LRS when the applied voltage sweeps backward to $0\ \text{V}$ (arrow 2). Subsequently, as the applied voltage increases from $0\ \text{V}$ to $4\ \text{V}$ (arrow 3), a negative differential resistance (NDR) region between $1.7\ \text{V}$ and $2.2\ \text{V}$ appears, indicating that the resistance of device switches from LRS to HRS. Such a transition is corresponding to the "RESET" process. When the positive voltage sweeps backward to $0\ \text{V}$ (arrow 4), the HRS is remained. *Viz.*, the device behaves as a bipolar memristor.^{22,23} It is switched ON ("SET" process) only by applying a negative bias ($< -3\ \text{V}$), and it is switched OFF ("RESET" process) only by applying a positive bias ($> 2.2\ \text{V}$). Besides, we measure the endurance performance of the AlN/n-GaN MIS device. The absolute current of LRS and HRS versus the number of switching cycles at $-0.5\ \text{V}$ reading voltage is presented in Fig. 2(b). The inset shows the representative I - V curves of 100 sweeping cycles. As can be seen, the current of LRS and HRS deteriorates slightly when the sweeping number increases, which is ascribed to the dislocations in AlN/n-GaN material prepared by MOCVD. It is said that dislocations are the major leakage passages for

nitride materials.²⁴ Although the endurance performance of the AlN/n-GaN MIS device needs to be further improved, the study confirms that it has reproducible bipolar resistive switching characteristics which can be applied in reproducible nonvolatile memory potentially.

In order to understand the resistive switching mechanism of the AlN/n-GaN MIS device, the "SET" process of I - V curve is replotted in double logarithmic scale, as shown in Fig. 3(a). It can be seen from the linear fitting results that the I - V curve of LRS nearly follows Ohmic law with a slope

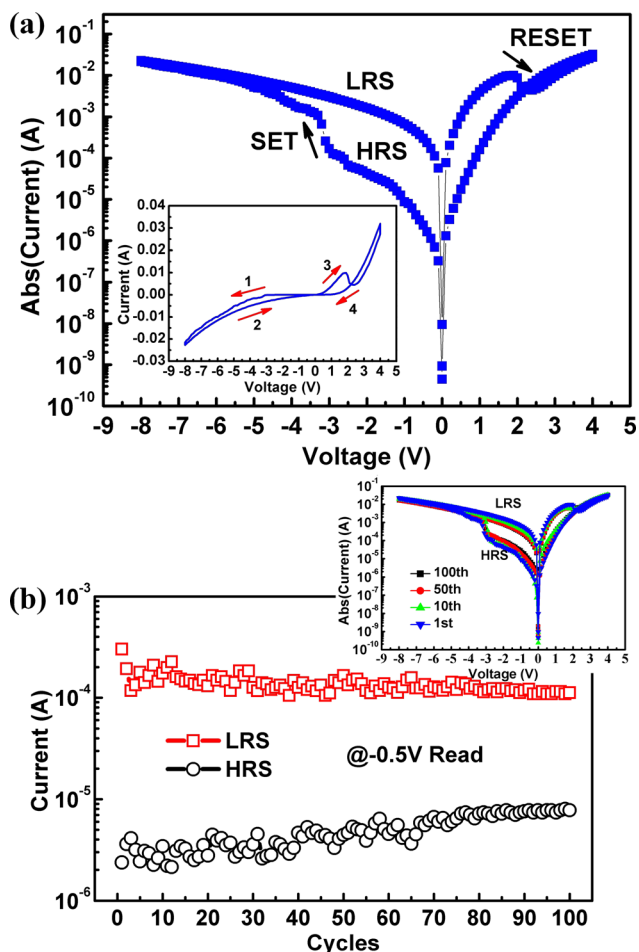


FIG. 2. (a) Typical I - V curve of the pristine AlN/n-GaN MIS device is shown in semi-logarithmic scale. The direction pointed by red arrows numbered 1 to 4 in inset is the sequence of sweeping voltage. (b) Endurance performance of the AlN/n-GaN MIS device. The inset shows the representative I - V curves of 100 sweeping cycles.

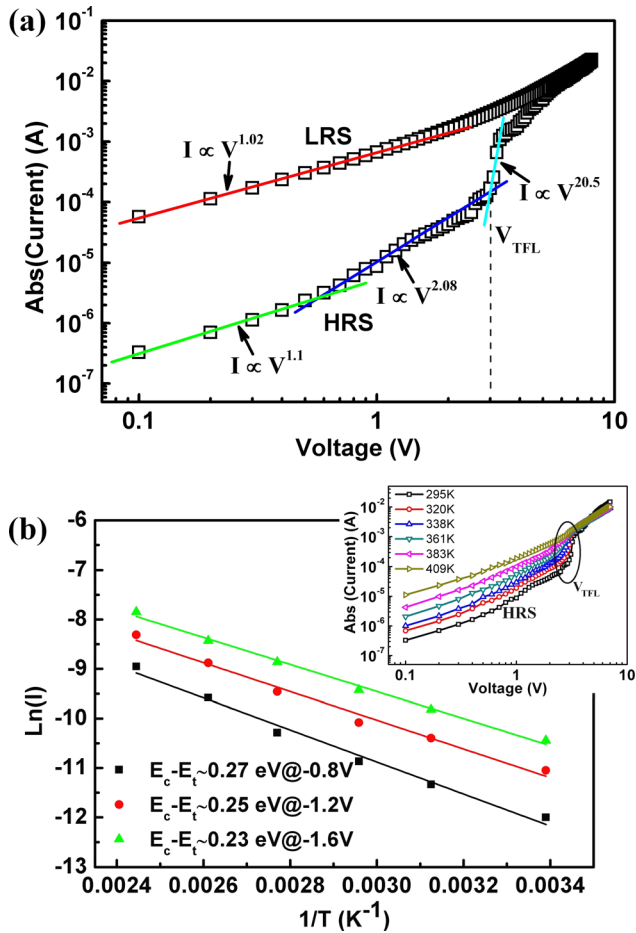


FIG. 3. (a) The linear fitting for the pristine I - V curve of "SET" process in logarithmic-logarithmic scale. (b) Arrhenius plots for the current-temperature curves at different bias. The inset shows the I - V curves of the HRS at "SET" process in logarithmic-logarithmic scale under different temperature.

of 1.02 ($I \propto V^{1.02}$) while the I - V curve of HRS is bounded by three limited curves in good accordance with the classical trap-controlled space charge limited current (SCLC) theory, which consists of three regions: the Ohmic region ($I \propto V$), the Child's law region ($I \propto V^2$), and the traps-filled-limit region including a voltage threshold (V_{TFL}) and a steep current rise.²⁵⁻²⁷ Based on trap-controlled SCLC theory, the resistive switching of our device should be related to the traps in the material. In our preparation of AlN/n-GaN material by MOCVD, the AlN was grown at low temperature (1100 °C) to prevent from damaging the n-GaN below. However, due to the weak surface mobility of Al adatoms, the quality of the AlN grown at low temperature was deteriorated and contained a large number of traps.²⁸ In order to confirm this viewpoint, the temperature-dependent I - V characteristics are measured. The trap energy level can be determined from the temperature-dependent current equation^{27,29}

$$I = I_0 \exp((E_t - E_c)/kT), \quad (1)$$

where k is the Boltzmann constant, E_t is the trap energy level, E_c is the conduction band lower edge, and T is the absolute temperature. As shown in the inset of Fig. 3(b), the current of the HRS during "SET" process under different temperature (from 295 K to 409 K) is presented in logarithmic-logarithmic

scale. The current of the HRS increases, and the steep current rise region becomes more and more gradual with the increase in the temperature, which indicates that the space charge limited effect is weakened at higher temperature. The reason can be ascribed to the increase of the thermal generated carriers and the weakened ability of the traps to capture carriers at higher temperature. The trap energy level can be obtained from the plot of $\ln(I)$ as a function of $1/T$, the slope of which is $(E_t - E_c)/k$. The $(E_c - E_t)$ which is on behalf of the thermal activation energy is calculated to be $\sim 0.25 \pm 0.02$ eV, from the temperature-dependent space charge limited current of the HRS, as shown in Fig. 3(b). This result closely approaches to the nitrogen vacancy energy level in AlN reported by Nepal *et al.*³⁰ Hence, E_t , associated to nitrogen vacancies locates below the E_c of AlN and therefore, the nitrogen vacancies could serve as electron traps and absorb injected electrons.^{31,32}

To further understand the mechanism of bipolar resistive switching in AlN/n-GaN MIS device, the traps (nitrogen vacancies) can be illustrated as potential wells. In wurtzite structure group-III nitrides, it is prone to generate spontaneous polarization because of the electronegativity difference between group-III and -V elements. The direction of the spontaneous polarization orientation of the group-III nitrides is relative to the III-polarity or N-polarity. It reported that the group-III nitrides grown by two-step method usually presented III-polarity, which formed spontaneous polarization with direction pointing in the opposite direction of c -axis.³³ Due to the spontaneous polarization field (P_{sp}) of AlN, the potential wells are tilted upward, as shown in Fig. 4(a). The energy band diagrams for bipolar resistive switching are shown in Figs. 4(b) and 4(c). Under reverse voltage, the applied electric field (E_{appl}) points to Ni electrode, which is opposite to P_{sp} and depletes the majority carriers (electrons) at the n-GaN space charge region and AlN/n-GaN interface. At the low E_{appl} , though the tilt of the potential wells is weakened to facilitate the transport of injected carriers, the injected carrier concentration from Ni electrode is lower than the thermal equilibrium concentration of the AlN, so the MIS device stands at the Ohmic region of HRS. With the increase of the E_{appl} , the electrons inject from the Ni electrode to n-GaN with the aid of the nitrogen vacancies. In this process, the potential wells tilt downward to the n-GaN so that the injected electrons can easily fill the nitrogen vacancies. The I - V characteristic undergoes a transition from the Ohmic region to space charge limited region. The trap-filled electrons make the electron concentration of AlN increase and thus its resistance drops. When the reverse voltage reaches the critical voltage ($V_{TFL} = -3$ V), the majority of the nitrogen vacancies are filled with electrons and form electron transport channel. At this moment, the injected electrons can pass through the AlN by trap-to-trap hopping under the E_{appl} , as shown in Fig. 4(b). Therefore, the current undergoes a steep rise, corresponding to the "SET" process. After the resistive switching, the MIS device keeps LRS with traps filled with electrons as long as the polarity of applied voltage is invariant. When the polarity of applied voltage is changed, majority of the carriers begin to accumulate at the interface of AlN/n-GaN. In this process, the E_{appl} is in the same direction of P_{sp} , which enhances the upward tilt of the potential

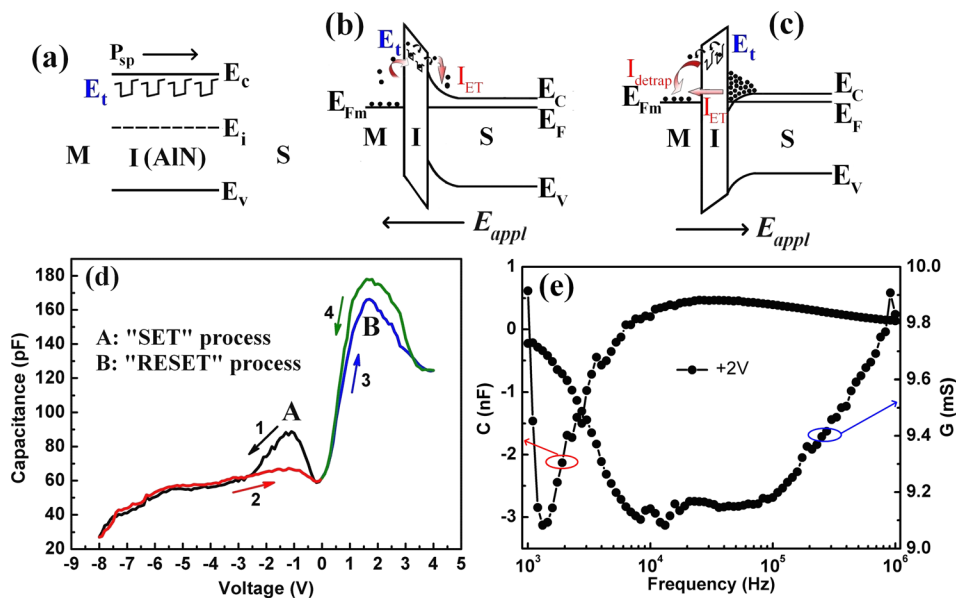


FIG. 4. (a) Schematic diagram of the trap structure under spontaneous polarization field of AlN. The energy band diagrams at (b) the "SET" process and (c) the "RESET" process. (d) C - V curve of AlN/n-GaN MIS device. (e) The frequency-dependent capacitance and conductance in the forward bias region.

wells. As a result, the trapped electrons can easily jump out of the potential wells while the electrons accumulated at the AlN/n-GaN interface in saturation regime are screening the spontaneous polarization in the AlN layer, which neutralizes their effect on refilling the emptied wells, as shown in Fig. 4(c). Without further electrons refilling, the NDR occurs between 1.7 V and 2.2 V during the electron detrapping from nitrogen vacancies, corresponding to the "RESET" process. At this moment, the small number of injected electrons from n-GaN, which corresponds probably to a thermionic assisted tunneling transport in forward biased Schottky junction Ni/AlN/n-GaN, can directly contribute to the current, regardless of the electron transport via the channel formed by potential wells. The bipolar resistive switching in essence is the formation/rupture of electron transport channel by trapping/detrapping electrons in nitrogen vacancies.

The electric transport mechanisms inferred from the I - V measurements can be also proved by capacitance-voltage (C - V) characteristic. The C - V curve is measured at 1 MHz using Agilent B1500, as shown in Fig. 4(d). The C - V measurement is in accordance with the I - V measuring sequence pointed by arrows numbered 1 to 4. As can be seen, in the range of 0 V to -3 V, the capacitance of the "SET" process (labeled A) increases first, which indicates the electrons trapping in nitrogen vacancies, and then decreases, which indicates the formation of the electron transport channel. The capacitance of the "RESET" process (labeled B) decreases at about 1.7 V, which corresponds to the detrapping process. To further confirm the process of charges detrapping from potential wells, the frequency-dependent capacitance and conductance is measured from 1 kHz to 1 MHz at +2 V, as shown in Fig. 4(e). Under low frequency, the capacitance C undergoes negative evolution that is probably a signature of the device discharge. At low frequency, the trapped electrons in the potential wells can follow the ac signal, and hence, their discharge under the applied constant +dc would be detectable and manifest with a decrease of the capacitance evolving even to negative value.¹⁸ While at higher frequency measurements, these electrons cannot follow the ac signal and result in less influence on the capacitance change. The small capacitance

dispersion at high frequency range from 50 kHz to 1 MHz could be probably linked to the bulk defects of AlN layer. According to the conductance G versus frequency characteristics, which show two transitions (Fig. 4(e)), Stoklas *et al.*³⁴ revealed that they are formed by two types of traps: surface state traps and bulk material traps, respectively. In accordance with this work, one deduces that the transition at high frequency is related to the traps in AlN layer.

In summary, we have obtained AlN/n-GaN material *in-situ* grown by MOCVD and fabricated MIS device based on Ni/AlN/n-GaN. The device presents obvious reproducible bipolar resistive switching characteristics. The study on its current transport indicates that the dominant conduction mechanism is based on trap-controlled SCLC theory. From Arrhenius plots, the trap energy level is calculated to be $\sim 0.25 \pm 0.02$ eV below E_c , which is formed by nitrogen vacancies. The observed bipolar resistive switching characteristics can be attributed to the nitrogen vacancies which form/rupture electron transport channel by trapping/detrapping electrons. In addition to the I - V characteristics and analyses, the mechanism is supported by admittance (C and G) characteristics.

This work was partially supported by the National Key Basic Research Program of China (Grant No. 2011CB301901), the National Natural Science Foundation of China (Grant Nos. 61322406, 61274038, 61204070, and 51472230), and the National High-Tech R&D Program (863, Grant No. 2011AA03A111).

¹G. I. Meijer, *Science* **319**, 1625 (2008).

²R. Waser and M. Aono, *Nat. Mater.* **6**, 833 (2007).

³M.-J. Lee, Y. Park, D.-S. Suh, E.-H. Lee, S. Seo, D.-C. Kim, R. Jung, B.-S. Kang, S.-E. Ahn, C. B. Lee, D. H. Seo, Y.-K. Cha, I.-K. Yoo, J.-S. Kim, and B. H. Park, *Adv. Mater.* **19**, 3919 (2007).

⁴M. Cavallini, Z. Hemmatian, A. Riminucci, M. Prezioso, V. Morandi, and M. Murgia, *Adv. Mater.* **24**, 1197 (2012).

⁵E. Matioli, S. Brinkley, K. M. Kelchner, Y. L. Hu, S. Nakamura, S. DenBaars, J. Speck, and C. Weisbuch, *Light Sci. Appl.* **1**, e22 (2012).

⁶U. Schwarz, *Nat. Photonics* **2**, 521 (2008).

⁷D. Li, X. Sun, H. Song, Z. Li, Y. Chen, H. Jiang, and G. Miao, *Adv. Mater.* **24**, 845 (2012).

- ⁸K. You, H. Jiang, D. B. Li, X. J. Sun, H. Song, Y. R. Chen, Z. M. Li, G. Q. Miao, and H. B. Liu, *Appl. Phys. Lett.* **100**, 121109 (2012).
- ⁹M. R. Holzworth, N. G. Rudawski, S. J. Pearton, K. S. Jones, L. Lu, T. S. Kang, F. Ren, and J. W. Johnson, *Appl. Phys. Lett.* **98**, 122103 (2011).
- ¹⁰D. Liu, N. Wang, G. Wang, Z. Shao, X. Zhu, C. Zhang, and H. Cheng, *Appl. Phys. Lett.* **102**, 134105 (2013).
- ¹¹M. Janousch, G. I. Meijer, U. Staub, B. Delley, S. F. Karg, and B. P. Andreasson, *Adv. Mater.* **19**, 2232 (2007).
- ¹²S. Seo, M. J. Lee, D. H. Seo, E. J. Jeoung, D. S. Suh, Y. S. Joung, I. K. Yoo, I. R. Hwang, S. H. Kim, I. S. Byun, J. S. Kim, J. S. Choi, and B. H. Park, *Appl. Phys. Lett.* **85**, 5655 (2004).
- ¹³D. H. Kwon, K. M. Kim, J. H. Jang, J. M. Jeon, M. H. Lee, G. H. Kim, X. S. Li, G. S. Park, B. Lee, S. Han, M. Kim, and C. S. Hwang, *Nat. Nanotechnol.* **5**, 148 (2010).
- ¹⁴Y. Ji, B. Cho, S. Song, T.-W. Kim, M. Choe, Y. H. Kahng, and T. Lee, *Adv. Mater.* **22**, 3071 (2010).
- ¹⁵S. Gao, C. Song, C. Chen, F. Zeng, and F. Pan, *Appl. Phys. Lett.* **102**, 141606 (2013).
- ¹⁶Y. Yang, P. Gao, S. Gaba, T. Chang, X. Pan, and W. Lu, *Nat. Commun.* **3**, 732 (2012).
- ¹⁷H. Y. Jeong, J. Y. Lee, and S.-Y. Choi, *Adv. Funct. Mater.* **20**, 3912 (2010).
- ¹⁸E. M. Bourim, Y. Kim, and D.-W. Kim, *ECS J. Solid State Sci. Technol.* **3**, N95 (2014).
- ¹⁹Y. Liu, T. P. Chen, P. Zhao, S. Zhang, S. Fung, and Y. Q. Fu, *Appl. Phys. Lett.* **87**, 033112 (2005).
- ²⁰X. Wu, K. L. Pey, N. Raghavan, W. H. Liu, X. Li, P. Bai, G. Zhang, and M. Bosman, *Nanotechnology* **22**, 455702 (2011).
- ²¹C. Chen, F. Pan, Z. S. Wang, J. Yang, and F. Zeng, *J. Appl. Phys.* **111**, 013702 (2012).
- ²²J. M. Tour and T. He, *Nature* **453**, 42 (2008).
- ²³D. B. Strukov, G. S. Snider, D. R. Stewart, and R. S. Williams, *Nature* **453**, 80 (2008).
- ²⁴D. W. Yan, H. Lu, D. S. Cao, D. J. Chen, R. Zhang, and Y. D. Zheng, *Appl. Phys. Lett.* **97**, 153503 (2010).
- ²⁵A. Lampert and P. Mark, *Current Injection in Solids* (Academic, New York, 1970).
- ²⁶M. A. Lampert, *Phys. Rev.* **103**, 1648 (1956).
- ²⁷Y. C. Yang, F. Pan, Q. Liu, M. Liu, and F. Zeng, *Nano Lett.* **9**, 1636 (2009).
- ²⁸Y. Chen, H. Song, D. Li, X. Sun, H. Jiang, Z. Li, G. Miao, Z. Zhang, and Y. Zhou, *Mater. Lett.* **114**, 26 (2014).
- ²⁹F. C. Chiu, H. W. Chou, and J. Y.-M. Lee, *J. Appl. Phys.* **97**, 103503 (2005).
- ³⁰N. Nepal, K. B. Nam, M. L. Nakarmi, J. Y. Lin, H. X. Jiang, J. M. Zavada, and R. G. Wilson, *Appl. Phys. Lett.* **84**, 1090 (2004).
- ³¹G. R. Fox and S. B. Krupanidhi, *J. Appl. Phys.* **74**, 1949 (1993).
- ³²Y. D. Xia, W. Y. He, L. Chen, X. K. Meng, and Z. G. Liu, *Appl. Phys. Lett.* **90**, 022907 (2007).
- ³³H. Morkoc, *Handbook of Nitride Semiconductors and Devices* (WILEY-VCH Verlag GmbH & Co. KGaA, Germany, 2008).
- ³⁴R. Stoklas, D. Gregusova, J. Novak, A. Vescan, and P. Kordos, *Appl. Phys. Lett.* **93**, 124103 (2008).